Available online at www.sciencedirect.com
ScienceDirect
Ceramics International 35 (2009) 2325–2328
CERAMICS INTERNATIONAL
www.elsevier.com/locate/ceramint

Characterization of Ni–Cu–Zn ferrite prepared from industrial wastes

Cheng-Hsiung Lin [a], Chih-Wei Wang [a], Yen-Pei Fu [b,*]

[a] Department of Graduate School of Optomechatronic and Materials, Wu-Feng Institute of Technology, Ming-Hsiung, Chiayi 621, Taiwan
[b] Department of Materials Science and Engineering, National Dong Hwa University, Shou-Feng, Hualien 974, Taiwan

Received 1 October 2008; received in revised form 30 November 2008; accepted 17 January 2009
Available online 6 February 2009

Abstract

We propose the distillation method to synthesize Ni–Cu–Zn ferrite powder and to recover nitric acid, using scrap iron and the waste solution of electroplating as the starting materials. It was found that the Ni–Cu–Zn ferrite powder prepared from industry wastes also showed the formation of cubic ferrite with a saturation magnetization (M_s) of 55,825 A m^2 g^{-1} and an intrinsic coercive force (Hci) of 579 A m^{-1}. For sintered Ni–Cu–Zn ferrite specimen, the toroidal specimen sintered at 950 °C for 2 h presented an maximum initial permeability (μ_i) of 176 at 28.3 MHz, a maximum quality factor (Q) of 32 at 3 MHz. The AC impedance measurements were performed by using impedance analyzer Solartron 1260. The semicircles in the impedance spectra shift to higher frequencies with increasing temperatures. The values of resistance (grain interior, grain boundary, and total) decreased with increasing temperatures. The semicircles of grain boundary and electrode are observed clearly. These data can be used to analyze typical the grain interior and the grain boundary resistance of Ni–Cu–Zn ferrite.

Keywords: A. Powder: chemical preparation; C. Magnetic properties; D. Ferrites; D. Spinels; E. Soft magnets

1. Introduction

Ni–Cu–Zn ferrite is usually used as magnetic material for multilayer chip inductors due to its lower sintering temperature and better properties at high frequency than Ni–Zn ferrite [1]. The conventional way of producing these materials is by the solid-state reaction of oxides/carbonates which are calcined at high temperatures [2,3]. Our group had investigated to synthesize Ni–Cu–Zn ferrite powder by hydrothermal process from the steel pickling liquor and the waste solution of electroplating for several years [4,5]. We attempted a new process (distillation method) to synthesize Ni–Cu–Zn ferrite powder and recovery nitric acid, using the scrap iron, electroplating waste solutions of nickel, zinc and copper as the starting materials. Nickel nitrate, copper nitrate and zinc nitrate waste solutions come from nickel, copper, and zinc electroplating plants, respectively. All these waste solutions must be treated to correspond to the environmental law and regulation in most industrialized countries. It involves high cost for the producers to treat these waste solutions. If we can effectively use recycled resources such as the scrap iron and the waste solutions of electroplating as the starting materials for Ni–Cu–Zn ferrite, then we can contribute to the protection of the earth and reduce the amount of industrial waste solutions.

2. Experimental procedures

The flow chart of experimental procedure is given in Fig. 1. Firstly, the concentration of cations in the electroplating waste solutions of nickel, copper, and zinc were analyzed by inductively coupled plasma (ICP). Secondly, the scrap irons and electroplating waste solutions were mixed together and heated until the scrape iron is completely dissolved in the mixed solution. The concentration of cations in the mixed solution was adjusted by adding the chemicals in accordance with ICP analysis. The distillation process involves heating the mixed solution consisting of the scrap iron, and electroplating waste solutions of nickel, zinc and copper. According to ion chromatography analysis, it was found that the condensate contained the nitrate ion. It is confirmed that these condensed liquid is nitric acid. Accordingly, we can recover the nitric acid from the distillation and recycle to use these nitric acids in other industry. During the distillation procedure, the great part of the mixed solution recovered in form of nitric acid and produced a

* Corresponding author. Tel.: +886 3 863 4209; fax: +886 3 863 4200.
E-mail address: d887503@alumni.nthu.edu.tw (Y.-P. Fu).

0272-8842/$34.00.
doi:10.1016/j.ceramint.2009.01.011

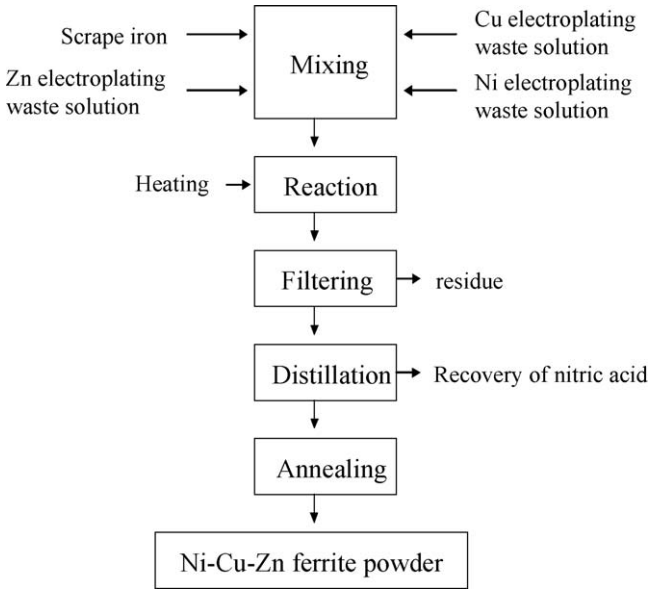

Fig. 1. Flow chart for preparation of Ni–Cu–Zn ferrite powder by distillation process from industrial wastes.

small part of residue. We can regard these residues as the precursor of Ni–Cu–Zn ferrite. Finally the Ni–Cu–Zn ferrite powder was obtained by annealing at 700 °C for 2 h. Then these ferrite powders were granulated and pressed into toroidal specimens under a uniaxial pressure of 1000 kg/cm^2. The toroidal specimens were then sintered at 950 °C for 2 h at a rate of 5 °C.

A computerized X-ray powder diffractometer (XRD) with Cu Kα radiation (XRD; Rigaku D/Max-II, Tokyo, Japan) was used to identify the crystalline phase. A vibrating sample magnetometer (VSM; Lake Shore 7407, Westerville, OH) was used to measure the saturation magnetization (M_s) and intrinsic coercivity (Hc) of Ni–Cu–Zn ferrite powder. Scanning electron microscopy (SEM; Hitachi S-3500H, Tokyo, Japan) was used to study the microstructure of Ni–Cu–Zn ferrite. The initial permeability (μ_i) and quality factor (Q) of sintered Ni–Cu–Zn ferrite were measured on an Hewlett-Packard 4194A impedance analyzer (Agilent, Santa Clara, CA) in the frequency range of 1 kHz–100 MHz; 15 turns of coil were wound around the sintered toroidal specimens. The impedance measurements were performed with an impedance analyzer SI 1260 (Solartron analytical, Hampshire, UK) over 1 Hz–10 MHz frequency range on isothermal plateaus half an hour long and the measurement temperature ranged from 250 °C to 350 °C with an increment of 50 °C.

3. Results and discussion

Fig. 2 shows the X-ray diffraction patterns of the annealed Ni–Cu–Zn ferrite powder and sintered Ni–Cu–Zn ferrite specimen. It revealed that annealed powders and sintered specimens contain only the spinel cubic ferrite. All the peaks in the pattern match well with the Joint Committee of Powder Diffraction Standard (JCPDS) card. No impurity phases can be detected in the X-ray pattern. The magnetization measurement

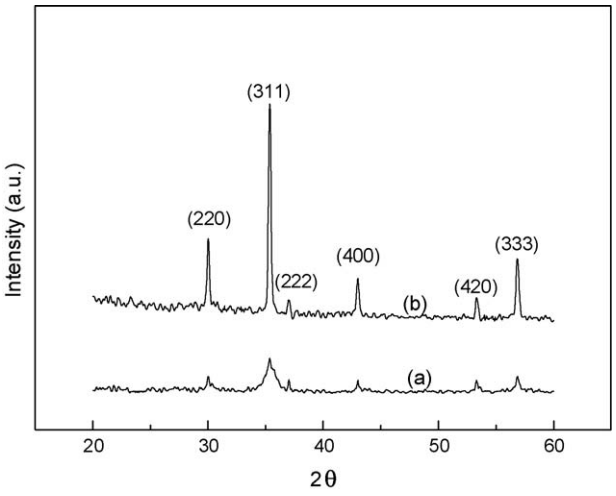

Fig. 2. XRD powder patterns of (a) annealed Ni–Cu–Zn ferrite powder, and (b) sintered Ni–Cu–Zn ferrite specimen.

for Ni–Cu–Zn ferrite powder prepared by distillation method was carried out using a vibrating sample magnetometer at room temperature with an applied magnetic field of 10 kOe to reach the saturation values. Fig. 3 shows hysteresis loops for annealed Ni–Cu–Zn ferrite powder. It indicates that the annealed Ni–Cu–Zn ferrite is a soft magnetic material, which reveals minimal hysteresis. The annealed Ni–Cu–Zn ferrite powder revealed the formation of cubic ferrite with a saturation magnetization (M_s) of 55825 Am^2 g^{-1} and an intrinsic coercive force (Hci) of 579 A m^{-1}.

It is well known that the permeability of spinel ferrite is strongly affected by saturation magnetization, crystal magnetization anisotropy, magnetostriction constant and internal stress. The equation of initial permeability is expressed as follows:

$$\mu_i = \frac{M_s^2}{aK + b\lambda\sigma}$$

where μ_i is initial permeability, M_s is saturation magnetization, K is crystal magnetic anisotropy, λ is magnetostriction constant,

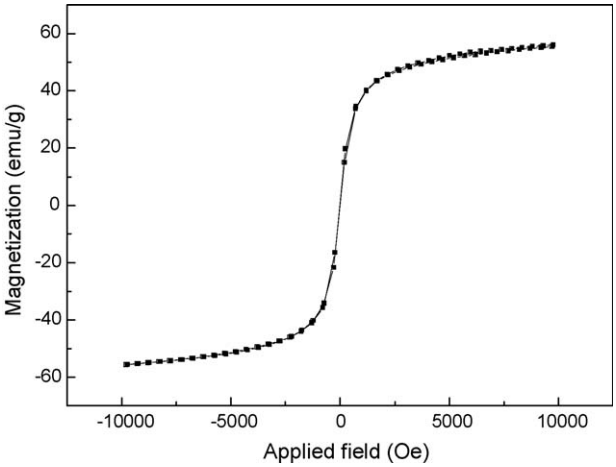

Fig. 3. Magnetization against applied field hysteresis curve for as-prepared Ni–Cu–Zn ferrite powder annealed at 700 °C for 2 h.

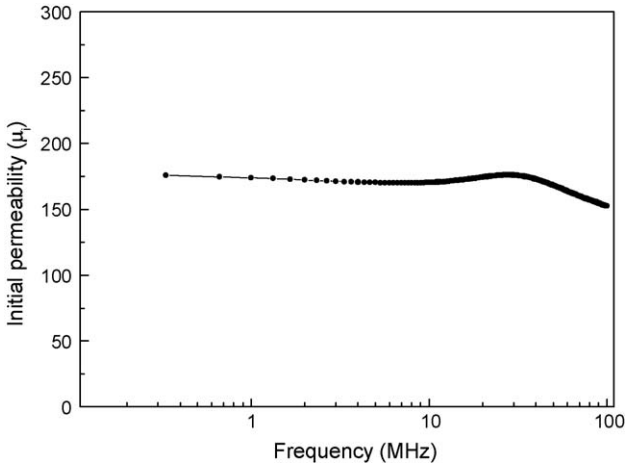

Fig. 4. Frequency dependence of initial permeability (μ_i) of Ni–Cu–Zn ferrite sintered at 950 °C for 2 h.

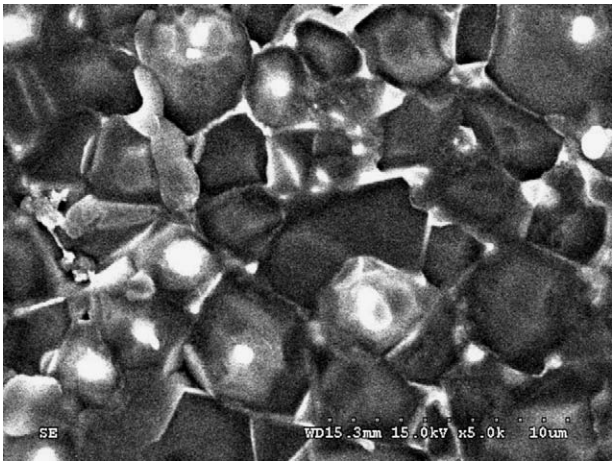

Fig. 6. Scanning electron micrograph of the sintered Ni–Cu–Zn ferrite specimen.

σ is internal stress, and a, b are constants [6]. If it is assumed that crystal magnetic anisotropy, magnetostriction, and internal stress are constant, the saturation magnetization will be predominant in this equation. Since the Ni–Cu–Zn ferrite powder annealed at 700 °C possessed a large saturation magnetization, we sintered this annealed Ni–Cu–Zn ferrite powder at 950 °C for 2 h. Figs. 4 and 5 show plots of the frequency dependence of initial permeability and quality factor for sintered Ni–Cu–Zn ferrite specimen. It is observed that the initial permeability shows the flat profile is from 1 kHz to 10 MHz and then rises to a maximum before falling rapidly to low values due to ferromagnetic resonance. The dispersion of initial permeability at low frequency is attributed to domain wall displacement. Ni–Cn–Zn ferrites are extensively used in multilayer chip inductors. For use in inductors, the initial permeability should remain fairly constant over certain frequency ranges. The initial permeability of 170 shows a flat profile from 0.2 MHz to 10 MHz. The maximum initial permeability of 176, was obtained at 28.3 MHz. On the other hand, the quality factor increases steadily from 1 kHz to 3 MHz and then falls gradually from 3 MHz to 30 MHz. The maximum quality factor value of 32 was obtained at 3 MHz. Fig. 6 shows the SEM images of the sintered Ni–Cu–Zn ferrite specimen prepared by distillation method from scrap irons and the waste solutions of electroplating. It indicates that particles are fairly uniform and the grains are connected to each other with a relative density above 90%. The grain sizes of the sintered Ni–Cu–Zn ferrite specimen are distributed in the range of 3–6 μm.

Fig. 7 displays the impedance diagram at 250 °C, 300 °C, and 350 °C for sintered Ni–Cn–Zn ferrite specimens. The semicircles in the impedance spectra shift to higher frequencies with increasing temperatures. The grain interior, grain boundaries and electrode–electrolyte interfaces are at high, middle, and low frequencies, respectively. The values of resistance (grain interior, grain boundary, and total) decreased with increasing temperatures. In this study, the semicircles of grain boundary and electrode are observed clearly. We can use these data to analyze typical the grain interior and the grain boundary resistance of Ni–Cu–Zn ferrite. The total resistance of electrolyte is given by

$$R_t = R_{gi} + R_{gb}$$

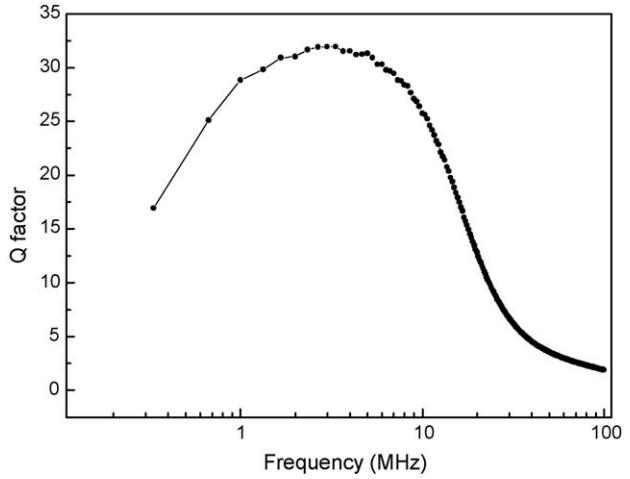

Fig. 5. Frequency dependence of quality factor (Q) of Ni–Cu–Zn ferrite sintered at 950 °C for 2 h.

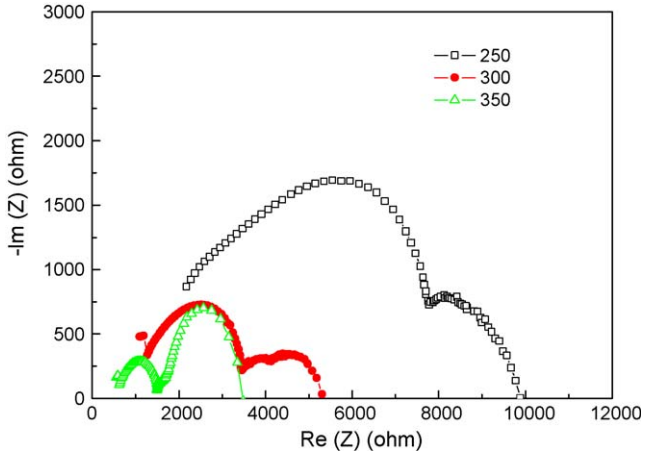

Fig. 7. Impedance plot of the sintered Ni–Cu–Zn ferrite specimen.

Table 1
Grain interior (σ_{gi}), grain boundary (σ_{gb}), and total conductivities (σ_t) of specimen for Ni–Cu–Zn ferrite.

Temperature (°C)	R_{gb}/R_t	σ_t (S/cm)	σ_{gi} (S/cm)	σ_{gb} (S/cm)
250	0.614	3.50×10^{-5}	9.05×10^{-5}	5.69×10^{-5}
300	0.776	7.17×10^{-5}	3.21×10^{-4}	9.23×10^{-5}
350	0.665	1.80×10^{-4}	5.50×10^{-4}	2.67×10^{-4}

where R_t is the total resistance, R_{gi} is the grain interior resistance, and R_{gb} is the grain boundary resistance [7]. Because of the character of the specimens, not all of these three arcs were observed at any temperature. In this study, the impedance measurements were performed from 1 Hz to 10 MHz frequency. According to the relevant literatures, it has been reported that the incomplete or small arc in the high frequency range can be attributed to the grain polarization. The broad arc in the middle frequency range is due to the grain boundary polarization. The spike appearing at low frequency is ascribed to the electrode polarization [8,9]. With the increase of temperature, the frequency range shifts to a higher value. One can distinguish the grain interior, the grain boundary, and the total resistances from the complex impedance plots. The relaxation frequency of the grain boundary is significantly lower at the intermediate temperature due to the higher capacitance. Nevertheless, we cannot distinguish the grain interior and the grain boundary conductivities at higher temperature because there is only one lower characteristic frequency term, from which we can only obtain the sum of the grain interior and the grain boundary resistance on the onset of the spike. Thus, de-convolution of the grain interior and the grain boundary contribution is found at low temperature (<500 °C). This data is insufficient to analyze the typical the grain interior and the grain boundary resistance of Ni–Cu–Zn ferrite. In order to evaluate the grain interior and grain boundary resistance at higher temperature, the grain boundary resistance (R_{gb}) was extrapolated from the total conductivity to estimate the bulk resistance ($R_b \sim R_t - R_{gb}$) [8,9]. The detailed conductivities properties of grain interior (σ_{gi}) and grain boundary (σ_{gb}) as a function of temperature are listed in Table 1. With the increase of temperature, the total conductivity increases to a higher value. Noticeably, the conductivity of the grain boundary has the same trend as that of the total. The resistance of grain boundary dominates the total resistance in sintered Ni–Cu–Zn ferrite. This is due to the fact that the grain boundary makes the primary contribution to the total in polycrystalline ferrite.

4. Conclusions

The aim of this study is to develop a new process to produce Ni–Cu–Zn ferrite powder and recovery nitric acid from scrap iron and waste solutions of electroplating. These Ni–Cu–Zn ferrite powders, when sintered at 950 °C for 2 h, exhibited fair initial permeability of 170 from 0.2 MHz to 10 MHz. Therefore, the sintered Ni–Cu–Zn ferrite showed an appropriate initial permeability suitable for multilayer-type chip inductor applications. The AC impedance measurements were performed to analyze the typical the grain interior and the grain boundary resistance of Ni–Cu–Zn ferrite. The values of resistance (grain interior, grain boundary, and total) decreased with increasing temperatures.

References

[1] H.M. Sung, C.J. Chen, W.S. Ko, H.C. Lin, Fine powder ferrite for multilayer chip inductors, IEEE Trans. Magn. 30 (1994) 4906–4908.
[2] P.S. Anil Kumar, J.J. Shrotri, S.D. Kulkarni, C.E. Deshpande, S.K. Date, Low temperature synthesis of $Ni_{0.8}Zn_{0.2}Fe_2O_4$ powder and its characterization, Mater. Lett. 27 (1996) 293–296.
[3] Y.P. Fu, C.S. Hsu, K.W. Tay, Preparation and magnetic properties of $Ni_{0.36}Zn_{0.64}$ ferrite from microwave-induced combustion, Jpn. J. Appl. Phys. 1 44 (2005) 1254–1257.
[4] M. Fjimotou, K. Hoshi, M. Nakazawa, S. Sekiguchi, Cu multiply twinned particle precipitation in low-temperature fired Ni–Zn–Cu ferrite, Jpn. J. Appl. Phys. 1 32 (1993) 5532–5536.
[5] Y.P. Fu, Characterization of Ni–Cu–Zn ferrite prepared from steel pickling liquor and waste solutions of electroplating, J. Am. Ceram. Soc. 89 (2006) 3547–3549.
[6] C.W. Liu, Y.P. Fu, C.H. Lin, Ni–Cu–Zn ferrite powder prepared from steel pickling liquor and waste solutions of electroplating, Jpn. J. Appl. Phys. 46 (2007) 1006–1008.
[7] J.X. Zhu, D.F. Zhou, S.R. Guo, J.F. Ye, X.F. Hao, X.Q. Cao, J. Meng, Grain boundary conductivity of high purity neodymium-doped ceria nanosystem with and without the doping of molybdenum oxide, J. Power Sources 174 (2007) 114–123.
[8] J.V. Herle, D. Seneviratne, A.J. McEvoy, Lanthanide co-doping of solid electrolytes: AC conductivity behaviour, J. Eur. Ceram. Soc. 19 (1999) 837–841.
[9] J.V. Herle, R. Vasquez, Conductivity of Mn- and Ni-doped stabilized zirconia electrolyte, J. Eur. Ceram. Soc. 24 (2004) 1177–1180.